HNUE JOURNAL OF SCIENCE DOI: 10.18173/2354-1059.2023-0061
Natural Sciences 2023, Volume 68, Issue 3, pp. 64-74
This paper is available online at http://stdb.hnue.edu.vn

SYNTHESIS AND CHARACTERIZATION OF CHITOSAN/CARRAGEENAN/POLYANILINE-BASED BIOCOMPOSITE AS LOVASTATIN CARRIER AND ITS DRUG RELEASE ABILITY IN BUFFER SOLUTIONS

Vu Thi Thu Thao[1], Nguyen Thi Hong Nhung[2], Vu Quoc Manh[2], Nguyen Ngoc Linh[2], Nguyen Thi Bich Viet[1] and Vu Quoc Trung[1]
[1]*Faculty of Pharmacy, Thanh Do University*
[2]*Faculty of Chemistry, Hanoi National University of Education*

Abstract. In this study, Chitosan/Carrageenan/Lovastatin/Polyaniline biocomposites (CsCLP) with different polyaniline (PANi) concentrations (0-10%) were successfully synthesized via the solution blending method. The chemical structure, morphology, and thermal properties of lovastatin-carried biocomposites were characterized by Fourier Transform Infrared (FTIR) spectroscopy, Field emission scanning electron microscope (FESEM), and Differential Scanning Calorimetry (DSC). The results revealed that among the CsCLP biocomposites synthesized, the sample CsCLP1955 with 5% wt. of PANi possessed the best dispersion of lovastatin (with the smallest particle size) in the composites. It also showed the smallest melting point (164.8^{o}C) and the most uniform morphology. The ability of biocomposites to release lovastatin in buffer solutions was investigated by UV-Vis spectroscopy analysis. It was found that this ability increased with the presence and the content of PANi in the composites. In the pH 2.0 buffer solution, the released lovastatin content reached 61.7 - 74.3% after 30 hours of testing, whereas in the pH 7.4 buffer, it was slightly better, at 68.5 - 78.1%, with the optimized ratio of PANi of 5% wt.

Keywords: Chitosan/Carrageenan/PANi/Lovastatin biocomposites, lovastatin release.

1. Introduction

Lovastatin (Lov) is a natural product derived from certain species of fungi through fermentation [1] that can effectively inhibit the activity of the enzyme hydroxyl methyl glutaryl CoA (HMG-CoA reductase) and is widely used as a hypercholesterolemia drug. Lov is rapidly absorbed in the small intestine when taken orally. Plasma concentrations of Lov reach a maximum within 4 hours with a half-life, $t_{1/2}$, of 3 hours and low bioavailability of 5 % [2] due to its poor aqueous solubility.

Received September 18, 2023. Revised October 23, 2023. Accepted October 30, 2023.
Contact Vu Quoc Trung, e-mail address: trungvq@hnue.edu.vn

In an attempt to achieve optimal absorption by the human body as well as bioavailability of the drugs during treatment, researchers focus on developing suitable and feasible methods and technologies that allow for increasing the aqueous solubility and dissolution rate of the drug. One of the most studied techniques is the preparation of drug-carrying polymeric nano- or micro-particles to control drug release. For this purpose, a wide range of polymers such as polymethacrylate (used as an excipient, Eudragit) [3], poly(lactic-co-glycolic) acid (PLGA) [4], polyaniline (PANi) [5-11], polycaprolactone (PCL) and polyethylene oxide (PEO) [12] have been investigated for their biocompatibility as well as their ability to control drug release from composite materials.

Suhair *et al.* tried to increase the dissolution rate of Lov by preparing polymeric microparticles via the coacervation phase separation method. The optimum microparticles were prepared using Eudragit L100 as polymer, ethanol as solvent, Lov: polymer ratio of 1: 2, and SDS surfactant in a concentration of 0.25 %, which resulted in an enhanced drug release of 5 folds [3]. Kelly A. Langert *et al*. prepared Lov-encapsulated PLGA nanoparticles at two drug-loading contents of 6.26 % and 25.0 % using an oil-in-water emulsion technique. It was reported that these nanoparticles could be an effective alternative strategy for local Lov delivery in the treatment of inflammatory demyelinating diseases [4].

In addition to that, polyaniline, a conducting polymer well known for its versatile properties such as anti-corrosion, supercapacitors, biosensors, etc. has been recently studied for its medical application, especially as a drug carrier in drug delivery systems. Regarding the biocompatibility of single PANi nanomaterials as a drug carrier, Zhang *et al*. investigated PANi nanomaterials with high (M_w~ 48,000 g/mol) and low (M_w~ 4000 g/mol) molecular weights and reported that the toxicity of PANi decreased as its molecular weight increased, in other words, PANi with higher molecular weights may have better biocompatibility [5]. However, most studies on PANi-based drug delivery systems focused on hollow nanoparticles or hydrogels as carriers of active pharmaceutical ingredients like curcumin [6], safranin [7], or indomethacin [8], and mostly in the form of composites. Besides, Hussein Shokry *et al.* developed hybrid scaffolds comprised of mesoporous silica nanoparticles embedded in a fiber matrix of polylactic acid-polyaniline. These scaffolds were shown to be biocompatible, electroactive, and effective at delivering and controlling cell-targeted drug release [9]. Yang *et al*. prepared graphene oxide (GO)-Fe_3O_4-PANi nanoparticles (NPs), another hybrid composite with magnetic properties, and studied its ability to carry and release platinum drugs in drug delivery systems for cancer therapies with two platinum complexes carboplatin (CBP) and oxaliplatin (OXP) as drug models. The results indicated that the releases of CBP and OXP from GO-Fe_3O_4-PANi NPs were affected by the pH, dose, and temperature. It was also reported that this material was biocompatible because almost no toxicity was observed in the testing range of concentration from 1 to 125 µg/mL and therefore it can be a great contribution to advances in cancer treatment [10].

On the other hand, a potential way to enhance the biocompatibility of drug carriers in drug delivery systems is preparing these carriers from biomaterials or combining biomaterials with polymers possessing desired properties such as PANi, polyhydroxyalkonate (PHA), polylactic acid (PLA), etc. In this direction, Minisy *et al.*

incorporated chitosan, a bio-based material, into a polymeric PANi matrix to produce chitosan/polyaniline-based nanofibrous composites via an *in situ* oxidative polymerization of aniline in the presence of chitosan. The release of ketoprofen (KP) was then studied and found to be linear with time in aqueous buffer solutions simulating gastric juice (pH 2.0), small intestinal fluid (pH 6.7), and colon fluid (pH 7.4), and increased with the pH of the medium [11]. In another work by Thach Thi Loc and co-workers [12], the alginate/chitosan/lovastatin composite (ACL) films were prepared with the presence of compatibilizers such as PEO and PCL at different contents (3-10%). The effect of compatibilizers and their contents on the *in vitro* release of Lov from ACL films was investigated. The results showed that Lov release could be controlled by the addition of compatibilizers, and the released Lov content from the ACL containing PEO was higher than that from the ACL film with PCL.

Recently, Cs and Carr have been widely used for fabricating drug carriers thanks to their good biocompatibility. However, their abilities to carry and release drugs as well as some physicochemical properties are still limited. To improve these properties, we try to combine them with PANi. To the best of our knowledge, no study has been reported on the Cs/Carr/PANi biocomposite as a Lov carrier. In this work, we aim to *(i)* synthesize and characterize Lov-carrying chitosan/carrageenan/PANi composites at different PANi concentrations (0-10 %); *(ii)* evaluate the effect of PANi on the Lov release from the composites in two pH buffer solutions (pH 2 as in the stomach and 7.4 as in the blood).

2. Content

2.1. Chemicals and experimental methods

**** Chemicals***

Carrageenan (Carr) (in powder; containing ≤ 2 % sodium, ≤ 3.5 % calcium, ≤ 11 % potassium; pH (1.5 % in H_2O) of 7.5–10.5; predominantly κ-Carr and a small amount of λ-Carr), chitosan (Cs) (medium viscosity, 200 - 400 mPa.S), and aniline are provided by Aladdin (China); dry powder lovastatin (≥ 98%) purchased from Rhawn (China). Other chemicals such as C_2H_5OH, HCl, KCl, CH_3COOH, KH_2PO_4, Na_2HPO_4, CH_3COONa, $(NH_4)_2S_2O_8$ were of analytical grades.

**** Synthesis of lovastatin-carrying chitosan/carrageenan/PANi biocomposites with variable content of PANi***

The chitosan/carrageenan/PANi biocomposites carrying Lov were prepared by the solution blending method. The content of PANi varied from 3 to 10% while keeping constant the concentrations of Carr, Cs, and Lov. In the first beaker, Carr was dissolved in water (Carr/water ratio = 1 g/ 200 mL) using a magnetic stirrer. The solution was then heated to 80^oC for 30 minutes and allowed to cool down to obtain solution A. In the second beaker, Cs was dissolved in a 1% acetic acid solution (Cs/acetic acid ratio = 1 g/ 200 mL) at room temperature under stirring for 20 minutes; aniline was then added followed by a 30-minute stirring; finally, ammonium persulfate (APS) was added at the molar ratio of APS/aniline of 1/1 and kept stirring for 1 hour to obtain solution B. In the third beaker, Lov was dissolved in ethanol using a magnetic stirrer to obtain solution C. In the next step, solution C was added dropwise into solution B via a glass burette while

stirring uniformly with a 20,000-rpm homogenizer to obtain solution D. Solution D was then allowed to stir on a magnetic stirrer for 1 hour. Next, solution A (Carr solution) was added to solution D while stirring uniformly with a 20,000-rpm homogenizer. The mixture obtained was stirred for 60 minutes with a magnetic stirrer and then centrifuged; the resulting solid was poured into a petri dish and lyophilized, yielding a brown powder. The compositions of the CsCLP composites synthesized are presented in Table 1.

The ratio of CS:Carr:Lov is 0.1: 0.9: 0.05 as presented in Ref. [13].

Table 1. Symbols and compositions of the CsCLP composite samples

No.	Symbols of the samples	Cs (g)	Carr (g)	Lov (g)	Anilin (mL)
1	CsCLP1950	0.1	0.9	0.05	0.00
2	CsCLP1953	0.1	0.9	0.05	0.03
3	CsCLP1955	0.1	0.9	0.05	0.05
4	CsCLP1957	0.1	0.9	0.05	0.07
5	CsCLP19510	0.1	0.9	0.05	0.1

**** Characterization of the CsCLP biocomposites***

FT-IR spectroscopy was used to determine the functional groups in the chemical structure of materials. The FT-IR spectra of the samples were recorded on a Nicolet iS10 Thermo Scientific and FTIR/NIR PerkinElmer spectrometer. Samples in powder form were mixed with KBr and pressed into pellets that were scanned in the range of 4000 cm^{-1} to 400 cm^{-1} with a resolution of 8 cm^{-1} and a scan number of 32 at room temperature.

FESEM images recorded on FESEM S-4800 Hitachi equipment were used to study the morphology of samples.

The thermal behaviors of CsCLP biocomposites were analyzed on a DSC-60 Shimadzu under a nitrogen atmosphere in the range from ambient temperature to 400^oC at a heating rate of 10^oC/minute.

Ultraviolet-visible (UV-Vis) spectroscopy was used to determine the content of lovastatin released from CsCLP biocomposites in different pH buffer solutions. These measurements were recorded on a UV-Vis S60 Libra Biochrom in the range of 200-400 nm.

**** Study of drug release***

The drug release from CsCLP composites was studied in buffer solutions simulating gastric juice (pH 2.0) and intestinal fluid (pH 7.4) at 37.0 ± 0.1 ^oC. Samples of known mass were added to a 300-mL beaker containing 200 mL of pH 2.0 or pH 7.4 buffers, respectively. The solutions were stirred continuously during the measurements. After each 1 hour, 5 mL of solutions were withdrawn and replaced by 5 mL of the fresh corresponding buffer to keep the volume of the studied solutions constant. The released drug content was determined by measuring the optical absorbance of Lov released from the CsCLP samples and using two calibration equations of Lov in the pH 2.0 buffer ($y = 2598.2x – 0.1468$, $R^2 = 0.9972$) and the pH 7.4 buffer ($y = 3978x – 0.1975$, $R^2 = 0.9985$). Each experiment was replicated three times.

2.2. Results and discussion

2.2.1. FTIR spectra of CsCLP

Figure 1 presents the FTIR spectra of Cs, Car, Lov, and CsCLP composites. It can be seen from the FTIR spectrum of pure Lov that the absorption bands were well attributed to characteristic groups in the Lov structure, such as 3644 cm^{-1} (stretching vibration of the –OH group), 1696 cm^{-1} (stretching vibration of the saturated –C=O in the lactone ring), and 1071 cm^{-1} (the –C–O– bond) [14]. With the spectrum of Carr, a vibration band at 847 cm^{-1} was assigned to the sulfate group at the C4 position of the galactose ring. The absorption bands at 3431 cm^{-1}, 1639 cm^{-1}, and 1077 cm^{-1} were attributed to valence vibration in the –OH, C=O, and –C–O– groups, respectively [15]. On the spectrum of Cs, all characteristic vibrational bands also appeared: 3360 cm^{-1} (vibration of –OH, –NH– groups, and intramolecular hydrogen bonds); 2920 cm^{-1}, 2966 cm^{-1} (symmetrical and asymmetrical stretching vibrations of C-H bonds); 1598 cm^{-1} (vibration bands of the N-acetyl and C=O bonds); 1028 cm^{-1} (asymmetrical deformation vibration band of the C–O–C group) [16]. With the FTIR spectrum of PANi, absorption bands characterized functional groups in the synthesized PANi structure, such as vibrations of the benzenoid ring at 1560 cm^{-1} and quinonoid ring at 1483 cm^{-1}; valence vibrations of the N–H secondary amine at 3436 cm^{-1}, and C– H of the phenyl ring at 2867 cm^{-1}; vibrations of N atoms bonded to quinonoid rings (N=quinoid=N) at 1294 cm^{-1}; vibrations of C atoms in aromatic rings bonded to diamine N atoms at 1240 cm^{-1}; and valence vibration of the C–N^+ group at 1097 cm^{-1} [17].

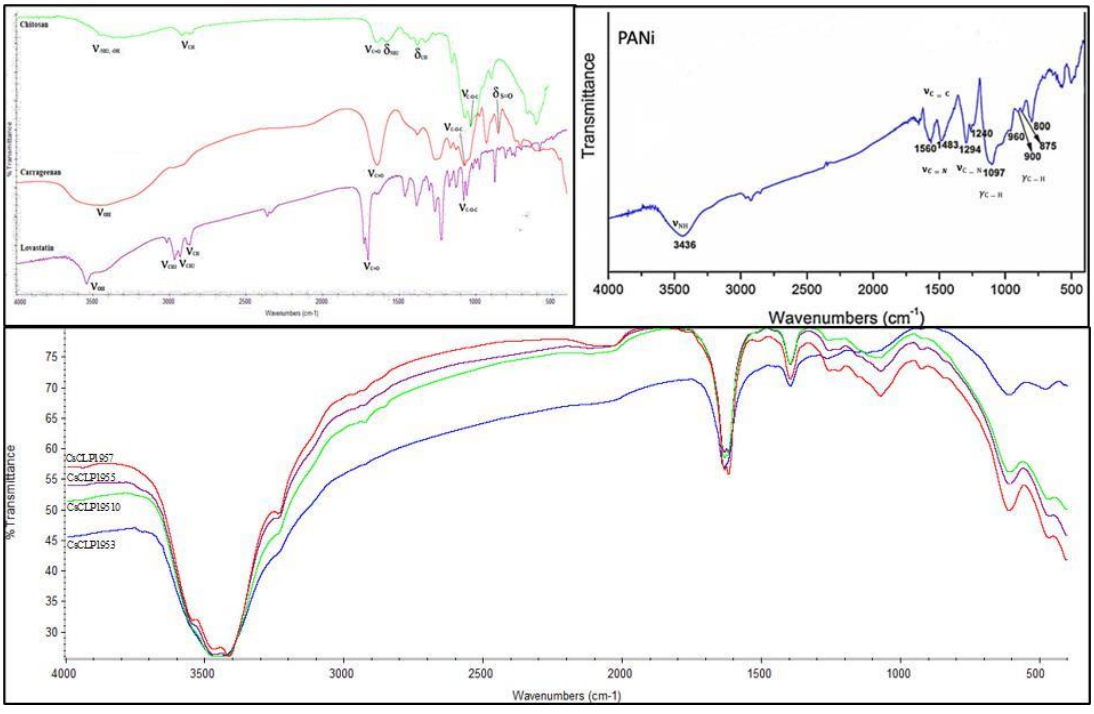

Figure 1. FTIR spectra of Cs, Carr, Lov, PANi, and CsCLP composites

Typical bands of all components (Cs, Carr, Lov, and PANi) can be observed on the spectra of CsCLP composites with slight shifts to the smaller wave number. This can be explained by strong interactions formed in the composite structure, such as dipole interactions between HSO_3^- groups in Carr and NH_3^+ groups in Cs protonated by acetic acid; hydrogen bonds between OH and NH_2 groups. The characteristic band at 3405 – 3460 cm^{-1} observed with CsCLP samples was attributed to valence vibrations of the O–H and N–H groups in Carr, Cs, and PANi. The 1615 – 1625 cm^{-1} band can be assigned to the C=C bonds of the quinonoid structure in PANI. The 1050 cm^{-1} band is assigned to the secondary and primary hydroxyl groups [18].

The small changes that occurred with the FTIR spectra of CsCLP composites also prove that all components in the composites are linked together through weak bonds (hydrogen bonds) without forming new chemical bonds. Therefore, the structure remains unchanged, resulting in stable physicochemical properties for each component. The change in PANi contents did not change the absorption spectra of the composites, proving that polymers interact well with each other and with the drug. The typical signals of all studied samples are listed in Table 2.

Table 2. Typical wave numbers of functional groups present in Cs, Carr, Lov, and CsCLP composites

	Cs		**Car**		**Lov**	**PANi**	**CsCLP 1953**	**CsCLP 1955**	**CsCLP 1957**	**CsCLP 19510**
νOH, NH2 νNH	3360		3431		3644	3436	3460	3410	3405	3450
νC=N	-	-	-	-	-	1560	1620	1620	1625	1615
νC=C(aren)	-	-	-	-	-	1483	1590	1580	1590	1575
νCH no	2920		2966		2966	2867				
νC=O	-		1639		1696	-	1638	1637	1637	1644
δNH	1598		-		-	1600	1638	1630	1635	1630
δCH	1376		1380		-	1097, 960, 900, 875	1223	1229	1216	1229
νC-O-C	1028		1077		1071	-	1042	1035	1042	1042
νS=O	-		847		-	-	-	-	-	-

2.2.2. Morphology of CsCLP composites

FESEM images of CsCLP composites with increasing content of PANi are presented in Figure 2. It can be seen from FESEM images that Lov particles were well dispersed into the Cs/Carr/PANi matrix. The sample CsCLP1955 depicted the best dispersion,

while other samples tended to form clusters with bigger sizes. This proves that the PANi content also affects the ability to disperse Lov particles into the polymer matrix. The tendency of the samples CsCLP1953 and CsCLP1957 to form clusters showed that PANi has formed electrostatic bonds with chitosan and dipole interactions between protonated amine groups in chitosan and sulfate groups in Carr, creating porous holes. This helps Lov penetrate the structure and form bonds with the matrix. In the 3 % PANi sample (CsCLP1953), a low concentration of PANi has caused a decrease in the porosity of the structure; therefore, the Lov particles are more difficult to disperse into the matrix. As for the 7 and 10 % PANi samples, they formed a dense network, linked to amine groups in Cs, reducing the groups capable of forming hydrogen bonds, so the number of hydrogen bonds between Lov and the composites was reduced. As a result, Lov particles aggregated together [19, 20].

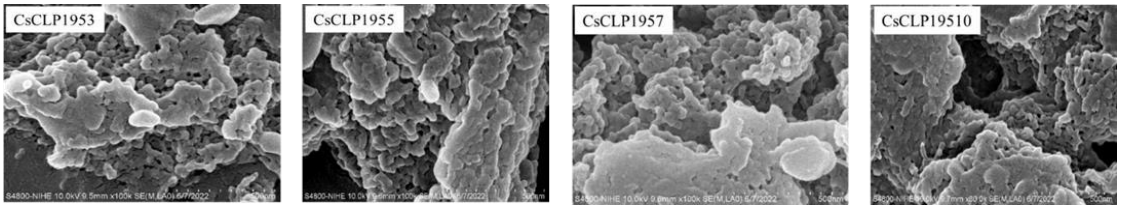

Figure 2. FESEM images of CsCLP composites with variable PANi contents

2.2.3. Thermal properties of CsCLP composites

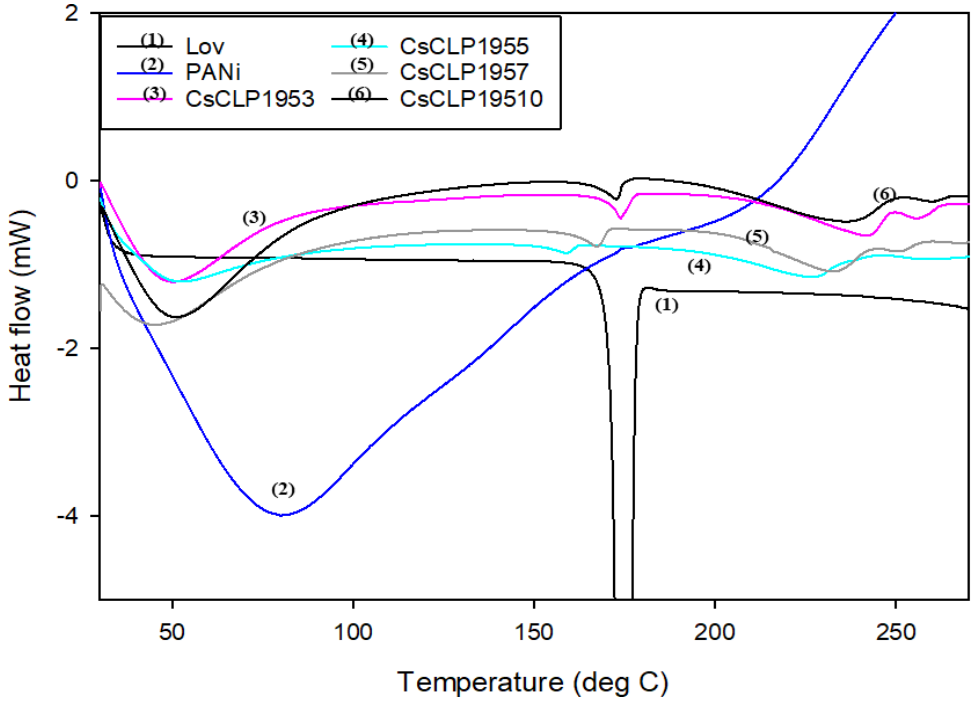

Figure 3. DSC diagrams of PANi, Lov, and CsCLP composites with variable PANi contents

Table 3. DSC parameters obtained with Lov, PANi, and CsCLP composites

Samples	1st endothermic peak (°C)	1st enthalpy (J/g)	2nd endothermic peak (°C)	2nd enthalpy (J/g)
PANi	74.1	-188.37	209.6	-64.51
Lov	-	-	174.3	-88.53
CsCLP1953	43.8	-170.76	168.9	-10.88
CsCLP1955	58.2	-79.86	164.8	-4.78
CsCLP1957	44.3	-62.75	166.6	-7.49
CsCLP19510	44.5	-179.32	167	-8.90

The DSC results are presented in Figure 3 and Table 3, which show that the Lov compound has an endothermic peak at 174.3°C corresponding to its melting point [21, 22, 23], while PANi demonstrates the first endothermic peak (assigned to its glass transition) at 74.1°C and the second one at 209.6°C (assigned to its melting point) [24]. When incorporating Lov and PANi into the chitosan/carrageenan composites, the melting point of Lov decreased to 164.8 – 168.9 °C (a decrease of 5 – 9°C). This can be due to the porous structure of the polymer matrix dispersing Lov particles to smaller sizes, reducing the crystallinity, and then reducing the melting point of Lov in the composites [18]. The CsCLP1955 sample showed the lowest melting point (164.8°C) among the CsCLP composites. This can be explained by the best dispersion of Lov into the composite, in other words, the smallest particle size. Especially, the first endothermic peaks of all composite samples range from 43.8°C to 58.2°C, probably attributed to the dehydration process of hydrophilic groups in Cs and Carr, in which the CsCLP1955 sample has the highest dehydration temperature. This may be because the PANi particles bonded well with chitosan and uniformly dispersed into the composite, increasing the dehydration temperature of the sample. In addition to that, the incorporation of Lov into the composites resulted in lower melting points of Lov compared to pure Lov, which can be explained by hydrogen bonds formed between Lov particles and polymers in the composites, leading to lower particle sizes [18, 19]. Once again, the lowest melting point of Lov in the CsCLP1955 sample proves the smallest particle sizes as well as the best dispersion, which is also consistent with the FESEM results.

2.2.4. Lovastatin release from CsCLP composites

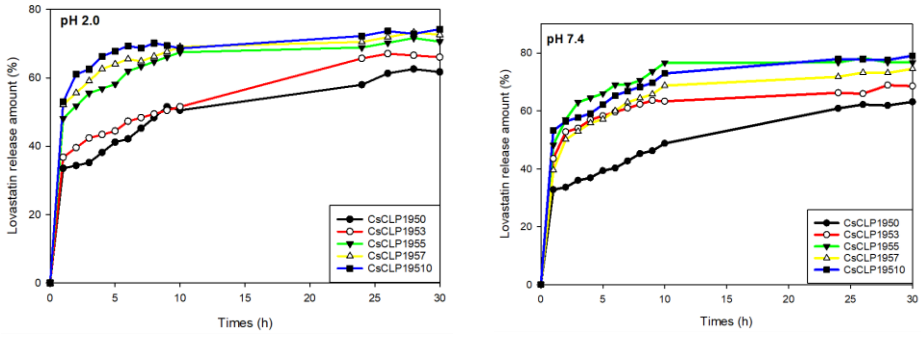

Figure 4. Plots of time-depending Lov amounts released from CsCLP composites at pH 2.0 and pH 7.4

The Lov releases from CsCLP composites at pH 2.0 and pH 7.4 are shown in Figure 4. It can be seen from Figure 4 that the releases of Lov from the composite without PANi (the CsCLP1950 sample) in both pH buffer solutions are lower than those from the composites with PANi. It is believed that the binding of PANi to the NH_2 groups in Cs reduces the hydrogen bonds in the composites; therefore, in buffer solutions, the composites easily swell and release faster and more effectively [11, 25]. In the pH 2.0 buffer solution, amine groups in Cs were protonated, and at the same time, H^+ ions also attacked and weakened the bonds between Cs and Carr, loosening these bonds and making them easier to release Lov particles [18, 19]. However, there were no certain rules for the samples. Based on the drug release results, it was clear that sample CsCLP1955 was the best choice. This is because Lov is better protected in the stomach since its release is slow at pH 2.0 while releasing well at pH 7.4 (intestinal pH) facilitates the absorption process into the blood. At neutral pH values, the amine groups tend to deprotonate, which may reduce the attraction between Lov molecules, thereby making Lov dissolve more easily. This enhances the release rate and ratio of Lov at pH 7.4 (higher than pH 2.0). In an acidic medium, the amine, imine, and hydroxyl groups of Cs, PANi, and Carr are protonated, thus binding well to Lov and making it less soluble in pH 2.0 buffer solution [11], resulting in its reduced release rate.

3. Conclusions

In this work, the chitosan/carrageenan/lovastatin/polyaniline biocomposites were successfully synthesized with an optimized content of PANi of 5 % wt., which was proved by the smallest melting point as well as the best dispersion of Lov particles in the composite. The influence of PANi on the ability to release Lov from these CsCLP composites was also evaluated using UV-Vis molecular absorption spectroscopy. The incorporation of PANi into the Cs/Carr/Lov composite enhanced the Lov release from the composite due to a decrease in the number of groups forming hydrogen bonds in Cs. Lov released well in neutral media (pH 7.4 simulating the intestinal fluid) by reducing the protonation of the functional groups in PANi and Cs.

REFERENCES

[1] Zhen-Jun Zhao, You-Zhao Pan, Qin-Jin Liu, Xing-Hui Li, 2013. Exposure assessment of lovastatin in Pu-erh tea. *International Journal of Food Microbiology*, Vol. 164, Iss. 1, pp. 26-31.

[2] Zolkiflee NF, Meor Mohd Affandi MMR, Majeed ABA, 2017. Lovastatin: history, physicochemistry, pharmacokinetics and enhanced solubility. *International Journal of Research in Pharmaceutical Sciences*, Vol. 8, Iss. 1, pp. 90-102.

[3] Suhair S. Al-Nimry, Mai S. Khanfar, 2016. Preparation and characterization of lovastatin polymeric microparticles by coacervation-phase separation method for dissolution enhancement. *Journal of Applied Polymer*, Vol. 133, pp. 43277-43286.

[4] Kelly A Langert, Bruktawit Goshu, Evan B Stubbs Jr, 2017, Attenuation of Experimental Autoimmune Neuritis with Locally Administered Lovastatin Encapsulating PLGA Nanoparticles. *J. Neurochem.,* Vol. 140, Iss 2, pp. 334-346.

[5] Yumei Zhang, Miaomiao Zhou, Chengfu Dou, Guodong Ma, Yin Wang, Ningchuan Feng, Wenping Wang, and Lanyun Fang, 2019. Synthesis and biocompatibility assessment of polyaniline nanomaterials. *Journal of Bioactive and Compatible Polymers*, Vol. 34, Iss. 1, pp. 16-24.

[6] Nilkamal Pramanik, Kingshuk Dutta, Ranjan K. Basu, Patit P. Kundu, 2016. Aromaticπ-conjugated curcumin on surface modified polyaniline/polyhydroxy alkanoate based 3D porous scaffolds for tissue engineering applications. *ACS Biomater. Sci. Eng.,* Vol. 2, Iss. 12, pp. 2365-2377.

[7] Qiuxi Fan, Kamalesh K. Sirkar, Bozena Michniak, 2008. Iontophoretic transdermal drug delivery system using a conducting polymeric membrane. *J. Membrane Sci.*, Vol. 321, Iss. 2, pp. 240-249.

[8] Lijuan Zhang, Zhiming Zhang, Paul A. Kilmartin, Jadranka Travas-Sejdic, 2011. Hollow polyaniline and indomethacin composite microspheres for controlled indomethacin release. *Macromol. Chem. Phys.,* Vol. 212, pp. 2674-2684.

[9] Hussein Shokry, Ulriika Vanamo, Oliver Wiltschka, Jenni Niinimäki, Martina Lerche, Kalle Levon, Mika Linden and Cecilia Sahlgren, 2015. Mesoporous silica particle-PLA–PANI hybrid scaffolds for cell-directed intracellular drug delivery and tissue vascularization. *Nanoscale*, Vol. 7, pp. 14434-14443.

[10] Yan-Fang Yang, Fa-Yan Meng, Xue-Hua Li, Ni-Ni Wu, Yong-Heng Deng, Li-Ying Wei, Xin-Peng Zeng, 2019. Magnetic Graphene Oxide-Fe3O4-PANI Nanoparticle Adsorbed Platinum Drugs as Drug Delivery Systems for Cancer Therapy. *J. Nanosci. Nanotechnol.,* Vol. 19, Iss. 12, pp. 7517-7525.

[11] Islam M. Minisy, Nehal A. Salahuddin, Mohamad M. Ayad, 2021. In vitro release study of ketoprofen-loaded chitosan/polyaniline nanofibers. *Polymer Bulletin*, Vol. 78, pp. 5609-5622.

[12] Thach Thi Loc, Thai Hoang, Nguyen Thuy Chinh, Le Duc Giang, 2018. The effects of the compatibilizers on the lovastatin release form the alginat/chitosan/lovastatin composite. *Vietnam Journal of Chemistry*, Vol. 56, Iss. 3, pp. 389-395.

[13] H. M. Hung, V. Q. Manh, V. T. T. Thao, D. T. P. Thuy, P. T. Dung, N. T. B. Viet, D. K. Linh, N. N. Linh, D. T. Y. Oanh, N. T. Chinh, T. Hoang, V. Q. Trung, 2022. Evaluation of the effect of the chitosan/carrageenan ratio on lovastatin release from chitosan/carrageenan based biomaterials. *Vietnam J. Chem.*, Vol. 60, No. S1, 72-78.

[14] D. S. Patel, R. M. Pipalya and Naazneen Surti, 2015. Liquisolid Tablets for Dissolution Enhancement of a Hypolipidemic Drug. *Indian J. Pharm. Sci.*, Vol. 77, Iss. 3, pp. 290-298.

[15] Vanessa Webber, Sabrina Matos de Carvalho, Paulo José Ogliari, Leila Hayashi, Pedro Luiz Manique Barreto, 2012. Optimization of the extraction of carrageenan from Kappaphycus alvarezii using response surface methodology. *Food Science and Technology (Campinas)*, Vol. 32, Iss. 4, pp. 812-818.

[16] Moacir Fernandes Queiroz, Karoline Rachel Teodosio Melo, Diego Araujo Sabry, Guilherme Lanzi Sassaki and Hugo Alexandre Oliveira Rocha, 2015. *Does the Use of Chitosan Contribute to Oxalate Kidney Stone Formation? Mar. Drugs.*, Vol. 13, Iss. 1, pp. 141-158.

[17] Nikolay Sirotkin and Anna Khlyustova, 2023. Plasma Synthesis and Characterization of PANI + WO_3 Nanocomposites and their Supercapacitor Applications. *J. Compos. Sci.*, Vol. 7, Iss. 4, pp. 174.

[18] Islam M. Minisy, Nehal A. Salahuddin, Mohamad M. Ayad, 2021. In vitro release study of ketoprofen-loaded chitosan/polyaniline nanofibers. *Polymer Bulletin*, Vol. 78, pp. 5609-5622.

[19] Hoang Thai, Chinh Thuy Nguyen, Loc Thi Thach, Mai Thi Tran, Huynh Duc Mai, Trang Thi Thu Nguyen, Giang Duc Le, Mao Van Can, Lam Dai Tran, Giang Long Bach, Kavitha Ramadass, C. I. Sathish & Quan Van Le, 2020. Characterization of chitosan/alginate/lovastatin nanoparticles and investigation of their toxic effects in vitro and in vivo. *Scientific Reports*, Vol. 10, Iss. 1, pp. 909.

[20] Dam Xuan Thang, Nguyen Thuy Chinh, Bach Long Giang, Hoang Tran Dung, C. I. Sathish, Ajayan Vinu, Thai Hoang, 2020. Characterization and Drug Release Control Ability of Chitosan/Lovastatin Particles Coated by Alginate. *J. Nanosci. Nanotechnol.*, Vol. 20, Iss. 12, pp. 7347-7355.

[21] Radhika Verma, Manju Nagpal, Thakur G. Singh, Manjinder Singh and Geeta Aggarwal, 2020. Improved Efficacy of Lovastatin from Soluplus-PEG Hybrid Polymer- Based Binary Dispersions. *Current Bioactive Compounds*, Vol. 16, Iss. 8, pp. 1164-1171.

[22] Agata Górniak, Maciej Gajda, Janusz Pluta, Hanna Czapor-Irzabek, Bożena Karolewicz, 2016. Thermal, spectroscopic and dissolution studies of lovastatin solid dispersions with acetylsalicylic acid. *Journal of Thermal Analysis and Calorimetry*, Vol. 125, Iss. 2, pp. 777-784.

[23] Dalia A Gaber, 2020. Nanoparticles of Lovastatin: Design, Optimization and in vivo Evaluation. *International Journal of Nanomedicine*, Vol. 15, pp. 4225-4236.

[24] CH. Srinivas, D. Srinivasu, B. Kavitha, N. Narsimlu, K. Siva Kumar, 2012. Synthesis and Characterization of Nano Size Conducting Polyaniline. *IOSR Journal of Applied Physics*, Vol. 1, Iss. 5, 12-15.

[25] Ana Luiza Cost Silva, J. C. Ugucioni, Silviana Corrêa, J. D. Ardisson, W. A. A. Macedo, J. P. Silva, A. A. C. Cotta, A. D. B. Brito, 2018. Synthesis and characterization of nanocomposites consisting of polyaniline, chitosan and tin dioxide. *Materials Chemistry and Physics*, Vol. 216, pp. 402-412.